VAND–TH–94–14–UPD
SHEP–95–08
hep–ph–9512229
December 1995

arXiv:hep-ph/9512229v1 5 Dec 1995

Updated: Higgs Mass Bounds Separate Models of Electroweak Symmetry Breaking

Marco A. Díaz
Physics Department
University of Southampton
Southampton, SO17 1BJ, U. K.

Tonnis A. ter Veldhuis and Thomas J. Weiler
Department of Physics & Astronomy
Vanderbilt University
Nashville, TN 37235, USA

ABSTRACT

Vacuum stability and metastability imply lower limits on the mass of the higgs boson in the Standard Model (SM). In contrast, we present an improved calculation of an upper limit on the lightest higgs mass in supersymmetric (susy) models, by summing to all orders in perturbation theory the leading and next–to–leading logarithms with a renormalization group equation technique, and by including finite two-loop QCD corrections. The improvement lowers the Minimal Susy Standard Model (MSSM) upper limit by about 10 GeV. The main uncertainty in each limit is the value of the top mass, which is now constrained by the recent Fermilab results. We study the possibility that these bounds do not overlap, and find that
(i) a mass gap emerges between the SM and the MSSM at $m_t \sim 175$ GeV for $\alpha_s(M_Z^2) = 0.118$ and at $m_t \sim 180$ GeV for more generous values $\sim (0.130)$ of α_s; and between the SM and the Minimal plus Singlet Susy Model [(M+1)SSM] if the independent scalar self–coupling of the latter is perturbatively small or if the $\tan\beta$ parameter is large; these gaps widen with increasing m_t;
(ii) the mass gap emerges with m_t 10 GeV lighter if only vacuum stability and not metastability is imposed;
(iii) there is no overlap between the SM and the MSSM bounds at even smaller values of m_t for the $\tan\beta$ value ($\sim$ 1–2) preferred in Supersymmetric Grand Unified Theories.
Thus, a measurement of the first higgs mass will serve to exclude either the MSSM/(M+1)SSM higgs sectors or the SM higgs sector. In addition, we discuss the upper bound on the lightest higgs mass in SUSY models with an extended higgs sector. Finally, we comment on the discovery potential for the lightest higgses in these models.
PACS numbers: 12.60Fr, 12.60Jv, 12.15Lk, 14.80Cp. 14.80Bn

1 Introduction

The simplest and most popular possibilities for the electroweak (EW) symmetry breaking sector are the single higgs doublet of the minimal Standard Model (SM), and the two higgs doublet sector of the Minimal Supersymmetric Standard Model (MSSM). Experimentally, very little is known about the higgs sector of the electroweak model. However, theoretically, quite a lot of higgs physics has been calculated. The electroweak symmetry–breaking scale is known: the vacuum expectation value (vev) of the complex higgs field Φ is $< 0|\Phi|0 >= v_{SM}/\sqrt{2} = 175$ GeV. This value is remarkably close to the top quark mass of $176 \pm 8 \pm 10$ GeV (which itself is very consistent with the values inferred from precision electroweak data, assuming the SM: $m_t = 164 \pm 25$ GeV in [1], and more recently, $m_t = 156 \pm 15$ GeV in [2]) announced by the CDF collaboration at Fermilab [3]. Higgs mass bounds have been calculated, including loop corrections. One aspect of the mass bounds [4] which we quantify in this paper is the following: inputing the CDF value for the top mass into quantum loop corrections for the symmetry–breaking higgs sector leads to mutually exclusive, reliable bounds on the SM higgs mass and on the lightest MSSM higgs mass [5, 6]. From this we infer that, *independent of any other measurement, the first higgs mass measurement will rule out one of the two main contenders for the electroweak theory: the SM, with no new physics below* $\sim 10^{10}$ *GeV, or the MSSM with supersymmetry breaking scale* $M_{SUSY} \lesssim 1$ *TeV.* Here we improve our previous calculation [5] of the renormalized MSSM higgs mass by including two-loop QCD corrections and then summing to all orders in perturbation theory the leading and next–to–leading logarithms with a renormalization group equation (RGE) technique [7, 8]. We also use the improved stability [6, 9] and metastability [10] lower bounds on the SM higgs mass (which we summarize in §2).

In the limit where the masses of the pseudoscalar, heavy and charged Higgs bosons (these are m_A, m_H and $m_{H^\pm}$, defined in §3) are large compared to M_Z (of the order of a TeV for example), the Feynman rules connecting the light Higgs in the MSSM to ordinary matter are approximately equal to the SM Feynman rules[11]. Therefore, in this limit, the MSSM light Higgs looks very much like the SM Higgs in its production channels and decay modes; the only difference, a vestige of the underlying supersymmetry, is that the constrained higgs self–coupling requires the MSSM higgs to be light, whereas SM vacuum stability requires the SM higgs to be heavy. Thus, *may only be possible to distinguish between the SM higgs and the lightest higgs of MSSM (with* $M_{SUSY} \lesssim 1$ *TeV) by their allowed mass values.* We demonstrate these allowed mass values in our Figures 1 and 2. Furthermore, the mass of the lightest MSSM higgs rises toward its upper bound as the "other" higgs masses are increased. [1] Thus, for masses in the region where the SM lower bound and the MSSM upper bound overlap, the SM higgs and the lightest MSSM higgs may not be distinguishable by branching ratio or width measurements [13]. Only if the two bounds are separated by a gap is this ambiguity avoided.

In the SM and even in supersymmetric models the main uncertainty in radiative corrections is the value of the top mass. With the announcement of the top quark mass, this

[1] The saturation of the MSSM upper bound with increasing "other" higgs masses is well known in tree–level relations (the bound $m_h \leq M_Z|\cos(2\beta)|$ approaches an equality as higgs masses increase) [12]. The MSSM upper bound still saturates with increasing "other" higgs masses even when one–loop corrections are included.

main uncertainty is greatly reduced. *The radiatively corrected observable most sensitive to the value of the top mass is the mass of the lightest higgs particle in susy models* [14]: for large top mass, the top and scalar–top ($\tilde{t}$) loops dominate all other loop corrections, and *the light higgs mass-squared grows as* $m_t^4 \ln(m_{\tilde{t}}/m_t)$. [2] We quantify this large correction, including two-loop QCD corrections and summing to all orders in perturbation theory the leading and next-to-leading logarithms, in §3.

In addition to contrasting the MSSM with the SM, we also consider in §4 supersymmetric models with a non-standard Higgs sector, in particular the Minimal–plus–Singlet Susy Standard Model [(M+1)SSM] containing an additional SU(2) singlet, and the low energy effective theory of SUSY models with a strongly interacting electroweak sector. A discussion of supersymmetric grand unified theories (susy GUTs) is put forth in §5; susy GUTs impose additional constraints on the low energy MSSM, leading to a lower upper bound on the lightest higgs mass. The discovery potential for the higgs boson is analyzed in §6, and conclusions are presented in §7.

2 Standard model vacuum stability bound

It has been shown that when the newly reported value of the top mass is input into the renormalized effective potential for the SM higgs field, the broken–symmetry potential minimum remains stable when the renormalization scale is taken all the way up to the Planck mass only if the SM higgs mass satisfies the lower bound constraint [9]

$$m_H > 139 + 2.1(m_t - 176) - 4.5(\frac{\alpha_s - 0.118}{0.006}), \;\; \Lambda = 10^{19}\text{GeV}. \tag{1}$$

In this equation, mass units are in GeV, and α_s is the strong coupling constant at the scale of the Z mass. The accuracy of the bound is estimated to be $\sim 5 - 10$ GeV. A similar but slightly lower bound is found in ref. [6]:

$$m_H > 136 + 1.92(m_t - 176) - 4.25(\frac{\alpha_s - 0.118}{0.006}), \;\; \Lambda = 10^{19}\text{GeV}, \tag{2}$$

valid in the range 150 GeV $< m_t <$ 200 GeV. These equations are the result of an analysis of the one-loop SM effective potential using two loop beta functions and the appropriate matching conditions. Here the estimated accuracy is $\lesssim 3$ GeV from the theoretical calculation, and $\lesssim 1$ GeV from the linear fit resulting in eq. (2).

The definition of the SM which we use requires no new physics (i. e. a desert) "only" up to the scale $\Lambda \sim 10^{10}$ GeV. We use the m_H vs. m_t curves for various cut–off values in ref. [6] to determine the coefficient of the m_t term at $\Lambda \sim 10^{10}$ GeV; and we run the SM renormalization group equations (RGE's) to determine the coefficient of the α_s term at $\Lambda \sim 10^{10}$ GeV. The resulting lower bound for $\Lambda \sim 10^{10}$ GeV is

$$m_H > 131 + 1.70(m_t - 176) - 3.47(\frac{\alpha_s - 0.118}{0.006}), \;\; \Lambda = 10^{10}\text{GeV}. \tag{3}$$

[2] It is not hard to understand this fourth power dependence; the contribution of the top loop to the SM higgs self energy also scales as m_t^4. However, in the SM the higgs mass is a free parameter at tree–level, and so any radiative correction to the SM higgs mass is not measurable. In contrast, in the MSSM the lightest higgs mass at tree–level is fixed by other observables, and so the finite renormalization is measurable.

The accuracy of this bound should approximate that of eq. (2), $\lesssim 4$ GeV. Because the parameter space for a smaller SM desert is necessarily contained within the parameter space for a larger SM desert, a smaller desert implies weaker constraints on the model; accordingly, we see that the lower bound on the higgs mass relaxes when the cut–off for new physics is reduced. In fact, it has been pointed out [9, 6] that the discovery of a higgs with low mass would place an upper limit on the scale of new physics.

This lower mass bound and the related "triviality bound"[15, 16, 17] are based on the physical requirement that the running higgs self–coupling remains positive and finite up to the energy scale Λ. Below this energy scale Λ the SM is supposed to be valid. If the higgs boson mass, given by $\sqrt{2\lambda}v_{SM}$, is too small compared to the top quark mass, then the running higgs self–coupling λ turns negative at a scale below the cut-off Λ[18]. On the other hand, if the higgs boson mass is too large, then the running self–coupling λ diverges at a scale below the cut–off Λ. Thus, for a given cut–off scale Λ and top quark mass m_t, the higgs mass is bounded from below by the vacuum stability bound, and bounded from above by the triviality bound. For large values of the cut–off, $\Lambda \gtrsim 10^{10}$ GeV, these bounds are only weakly dependent on the value of Λ[19, 6]. By comparing eqn. (3) with eqns. (1) and (2), we see that for a top quark mass $m_t = 176$ GeV and $\alpha_s = 0.118$, an increase in Λ from 10^{10} GeV to the Planck mass $\sim 10^{19}$ GeV raises the vacuum stability bound by only 5 to 8 GeV. To put it in simple terms: if the running self–coupling λ is going to diverge or become negative, it will do so at a relatively low energy scale.

It has been known for some time [20] that the SM lower bound rises rapidly as the value of the top mass increases through M_Z; below M_Z the bound is of order of the Linde–Weinberg value, ~ 7 GeV [21]. So what is new here is the inference from the large reported value for m_t that the SM higgs lower mass bound dramatically exceeds 100 GeV! Adding the statistical and systematic errors of the CDF top mass measurement in quadrature gives a top mass [3] with a single estimated error of $m_t = 176 \pm 13$ GeV. The D0 collaboration has also announced discovery of the top quark[23], with a top mass estimate of 199 ± 30 GeV, consistent with the (better–determined) CDF value. The main uncertainty in the SM vacuum stability bound remains the exact value of the top quark mass. The CDF one–sigma uncertainty of 13 GeV in the top quark mass translates into a 22 GeV one–sigma uncertainty in the bound of Eq. (3). The bound's dependence on the uncertainty in α_s, a better known parameter, is more mild.

It is possible that the observed vacuum state of our universe is not absolutely stable, but only metastable with a small probability to decay via thermal fluctuations or quantum tunneling. If metastability rather than absolute stability is postulated, then a similar but weaker bound results[24]. In an accurate calculation of this metastability bound, next–to–leading logs are included in the effective potential and one–loop ring graph contributions to the Debye mass are summed [10].

SM metastability bounds are given in ref. [10] in tabular form for $\alpha_s = 0.124$ and various values of Λ, and in analytic form for $\Lambda = 10^{19}$ GeV with various values of α_s. To derive the metastability bound for our cut–off value $\Lambda = 10^{10}$ GeV and various α_s values, we do the following: We first obtain the bound for $\alpha_s = 0.124$ and $\Lambda = 10^{10}$ GeV by extrapolating the

[3] A top mass limit independent of the top decay modes is provided by an analysis of the W boson width: $m_t > 62$ GeV at 95% confidence [22].

values given in Table 1. of [10]. The α_s–dependent term at $\Lambda = 10^{19}$ GeV is obtained from eqn. (30) in [10]. Based upon our experience with running the SM RGEs from $\Lambda = 10^{19}$ GeV down to $\Lambda = 10^{10}$ GeV for the SM stability bound, we note that the coefficient of the α_s–dependent term is renormalized down by 20% (compare eqn. (3) to eqns. (1) and (2)). So we reduce the coefficient of α_s by 20%. The change in the Higgs mass bound effected by this renormalization is small, ~ 1 or 2 GeV or less. The resulting metastability bound at $\Lambda = 10^{10}$ GeV is

$$m_H > 123 + 2.05(m_t - 176) - 3.9(\frac{\alpha_s - 0.118}{0.006})(\frac{m_t}{176}), \quad \Lambda = 10^{10}\text{GeV}. \tag{4}$$

According to eq. (2), the linear fit is valid to better than one GeV for $m_h > 60$ GeV, and the overall theoretical error is negligible compared to the experimental errors in the α_s and m_t values.

In our figures, we will present both the stability and the metastability lower bounds. The metastability bound is necessarily lower than the stability bound. A comparison of eqns. (3) and (4) shows that the ordering is maintained in the m_t–region of interest, below 200 GeV; beyond $m_t = 200$ GeV the fitted equations are no longer valid. The CDF top mass values including 1σ allowances are 163, 176, and 189 GeV. The vacuum stability bounds following from Eq. (3) for these top quark masses with $\alpha_s = 0.118$ are 109, 131, and 153 GeV, respectively, whereas the metastability bounds are 96, 123, and 150 GeV, respectively [4].

As is evident in eqns. (1), (2), (3), and (4), the vacuum stability and metastability bounds on the SM higgs mass are sensitive to the value of $\alpha_s(M_Z)$. We have taken $\alpha_s = 0.118$ (the central value in the work of [9]) to produce the bounds displayed in Fig. 1. The 1994 world average derived by the Particle Data Group [26] is 0.117 ± 0.005. The value derived from fitting SM radiative corrections to LEP/SLC precision electroweak data is $\alpha_s(M_Z) = 0.124 \pm 0.005$ in [2], and $\alpha_s(M_Z) = 0.122 \pm 0.005$ in [27]. Other LEP analyses, and deep inelastic leptoproduction (Euclidean) data extrapolated to the M_Z scale give lower values ~ 0.112; a comparison of low Q^2 deep–inelastic data to the Bjorken sum rule [28] yields [29] $\alpha_s(M_Z) = 0.116^{+0.004}_{-0.006}$. The LEP working group [30] quotes a world average of $\alpha_s(M_Z) = 0.120 \pm 0.006 \pm 0.002$, assuming the SM. If we use the generous value $\alpha_s = 0.130$, the stability bound on the SM higgs mass decreases by about 9 GeV for $m_t > 160$ GeV, and the metastability bound decreases by about 8 GeV.

The vacuum stability bound on the SM higgs mass rises roughly linearly with m_t, for $m_t \gtrsim 100$ GeV, whereas the upper limit on the lightest MSSM higgs mass grows quadratically with m_t. Therefore, for very large values of the top quark mass m_t, the two bounds will inevitably overlap. In addition, for low values of m_t the two bounds may overlap. For example, for very large or very small values of $\tan\beta$ the MSSM upper bound is at least M_Z, but the SM lower bound is only 60 GeV for $m_t = 130$ GeV[31]. However, for m_t heavy, but not too heavy, there may be no overlap. In what follows, we show that in fact for m_t around the value reported by the CDF collaboration, there is little ($\alpha_s = 0.130$) or no ($\alpha_s = 0.118$) overlap between the SM higgs mass lower bound and the MSSM upper bound. Thus, the

[4] LEP experiments have established the non–existence of the SM higgs particle below a mass value of 64 GeV [25].

first measurement of the lightest higgs mass will probably suffice to exclude either the SM higgs sector, or the MSSM higgs sector!

3 The lightest higgs in the MSSM

The spectrum of the higgs sector in the MSSM contains two CP–even neutral higgses, h and H, with $m_h < m_H$ by convention, one CP–odd neutral higgs A and a charged higgs pair $H^\pm$. A common convenience is to parameterize the higgs sector by the mass of the CP–odd higgs m_A and the vev ratio $\tan\beta \equiv v_T/v_B$. These two parameters completely specify the masses of the higgs particles at tree level

$$\begin{aligned} m^2_{H,h} = &\quad \tfrac{1}{2}(m^2_A + m^2_Z) \pm \tfrac{1}{2}\sqrt{(m^2_A - m^2_Z)^2\cos^2 2\beta + (m^2_A + m^2_Z)^2 \sin^2 2\beta} \\ m^2_{H^\pm} = &\quad\quad\quad

We use the diagramatic technique with an on-shell renormalization scheme to calculate the renormalized lightest MSSM higgs mass, m_h [7]. We include the full one–loop corrections from the top/bottom quarks and squarks, the leading–log corrections from the remaining fields (charginos, neutralinos, gauge bosons, and higgs bosons) [6], the dominant two–loop corrections, and the full momentum–dependence of the higgs self–energies. We then perform a Renormalization Group Equation (RGE) improvement [38] of these results in order to include the resummed leading and next–to–leading logarithms. The result is a highly accurate calculation of the lightest MSSM higgs mass, perhaps the most accurate available in the literature.

We find the renormalized neutral higgs masses by looking for the zeros of the determinant of the inverse propagator matrix, including the loop corrections [8]. The two solutions to

$$\Sigma^{\chi}_{11}(p^2)\Sigma^{\chi}_{22}(p^2) = \left[\Sigma^{\chi}_{12}(p^2)\right]^2, \tag{8}$$

are the pole higgs masses $p^2 = m_h^2$ and $p^2 = m_H^2$. The propagators are calculated in a basis in which the CP-even higgs fields χ_1 and χ_2 are unmixed at tree-level. We renormalize each matrix element of the inverse propagator matrix first, and later diagonalize it nonperturbatively. Furthermore, we keep the full momentum dependence of the self energies in eq. (8). This is equivalent to defining a momentum dependent mixing angle $\alpha(p^2)$. With this procedure, we avoid the introduction of a mixing angle counterterm, which allows us to calculate directly the renormalized mixing angle at the two physically relevant scales $\alpha(m_h^2)$ and $\alpha(m_H^2)$ [8].

Two–loop corrections are negative and decrease the upper bound of the higgs mass by several GeV [39]. We include the dominant two–loop corrections of ref. [39] which include the leading and next-to-leading logarithms. Finally, using an RGE technique, we extend the results of ref.[39] by summing to all orders in perturbation theory these leading and next–to–leading logarithm terms. In order to do this, we solve the two-loop RGE [40] with a supersymmetric boundary condition at the scale M_{SUSY} to obtain the quartic higgs self–coupling constant at the weak scale. In this way, the running higgs mass squared is equal to λv^2, where $v^2 = v_T^2 + v_B^2$ (v_T and v_B are the vevs of the two higgs doublets.). This RGE improvement[34, 39],

$$(\Delta m_h^2)_{RGE} = \lambda v^2 - M_Z^2 \cos^2 2\beta - (\Delta m_h^2)_{lnll}. \tag{9}$$

depends of course on the value of the top quark mass. Here $(\Delta m_h^2)_{lnll}$ contains the logarithmic part of the one– and two–loop corrections, the so–called leading and next–to–leading logarithms. For example, at $m_t \sim 176$ GeV, we find the RGE correction to be –2 to –3 GeV for large $\tan\beta$ and –5 to –7 GeV if $\tan\beta$ is small. We include this correction in all of our plots.

We choose m_A and all squark mass parameters to be large, equal to 1 TeV [7], in order to find the maximum light higgs mass. With respect to the squark mixing, we work in three

[6] Calculations of full one–loop corrections from all particles [37] have shown that finite (i. e. non–logarithmic) corrections due to loops with particles other than the top/bottom quarks and squarks are very small.

[7] We note that $\lesssim$ 1 TeV emerges naturally for the heavier superparticle masses when the MSSM is embedded into a GUT [41, 42, 43].

extreme scenarios:
(a) no mixing, i. e. , $\mu = A_t = A_b = 0$, where μ is the supersymmetric higgs mass parameter and A_i, $i = t, b$ are the trilinear soft supersymmetry breaking terms; and
maximal mixing
(b) with $\mu = A_t = A_b = 1$ TeV,
(c) and $\mu = -1$ TeV, $A_t = A_b = 1$ TeV.
We mention again that our chosen definition for the MSSM is the conventional one, with M_{SUSY}, all of the soft supersymmetry breaking terms, and μ, having a magnitude of at most 1 TeV. One of the motivations for this choice is that in supergravity models the electroweak symmetry can be broken radiatively without fine–tuning the initial parameters, if M_{SUSY} is not too large[44].

The resulting lightest higgs mass as a function of $\tan\beta$ is shown in Fig. 1 for the CDF central value of the top quark mass and the $\pm 1\sigma$ mass values. The accuracy of this bound can be estimated to be ~ 10 GeV, which is the difference between the one– and two–loop bound calculated before the RGE–resummation. For the case $\tan\beta \sim 1$, the SM lower bound and the MSSM upper bound are separated already at $m_t = 163$ GeV. Were if not for the SM metastability lower bound, the gap would exist for all values of $\tan\beta$. However, with the SM metastability bound, it is not until $m_t \sim 175$ GeV that a gap exists for all values of $\tan\beta$. In particular, for the preferred CDF value of $m_t = 176$ GeV, the two bounds do not overlap, making it possible to distinguish the SM and the MSSM solely on the basis of a determination of the higgs mass. Even for $m_t = 189$ GeV the gap is still increasing with increasing top mass, indicating that the eventual closing of the gap occurs at still higher values of m_t.

Should α_s turn out to be closer to 0.130 than to the value 0.118 assumed here, then the separation of the SM higgs mass region from the MSSM higgs mass region is not quite complete. We have seen that the stability and metastability lower bounds on the SM higgs mass decrease as α_s is increased. The MSSM mass upper bound also decreases with increasing α_s, but at a much smaller rate. We find that raising α_s from 0.118 to 0.130 shifts the MSSM higgs mass bound by -0.5 GeV for m_t =163 and by -0.8 GeV for m_t =189 GeV. The result is that the gap apparent for all values of $\tan\beta$ in the $\alpha_s = 0.118$, $m_t = 176$ GeV case (displayed in our Fig. 1b), remains a gap in the $\alpha_s = 0.130$ case only in the $\tan\beta \sim 1$ to 2 region. However, the overlapping mass region for the remaining $\tan\beta$ values is small. The region of overlap is interesting only if the observed higgs mass turns out to lie in this region. With a small overlap region, such an occurence is *a priori* unlikely. A further (interesting) complication is that the best fit value for α_s, when MSSM radiative corrections are assumed and fitted to precision data, is [45] $\alpha_s(M_Z) = 0.114 \pm 0.007$. This lower value suggests that it may be best to compare SM bounds with a given value assumed for α_s to MSSM bounds with a slightly lower value assumed for α_s.

In Fig. 1 we can see that scenario (c) gives us a significantly larger range of higgs mass values close to $\tan\beta \sim 1$. This can be understood in the $\tan\beta = 1$ approximation: there are non-leading logarithmic contributions to the higgs mass from loops involving the top quark and squarks that are proportional to powers of $(\mu - A_i)/m_t$ [34]. Also in Fig. 1 we see that scenarios (b) and (c) offers a larger value for the m_h maximum than does scenario (a), except for the region $\tan\beta \gg 1$. The reason is that among the additional light higgs mass terms in (b) is a negative term proportional to $-(\mu m_b/\cos\beta)^4$, which becomes large

[38] when $\tan\beta \gg 1$. More significant is the fact that the extreme values in (a), (b) and (c) yield a very similar absolute upper bound in the region of acceptable $\tan\beta$ values, thereby suggesting insensitivity of the MSSM upper bound to a considerable range of the squark mixing parameters.

In the literature there are three popular methods to calculate the renormalized higgs mass. These are the RGE technique, the effective potential method, and the diagramatic technique. It is informative to compare these techniques, and to point out the advantages of the approach we have undertaken. The RGE technique is used for example in ref. [40], where the leading and next-to-leading logarithms are summed to all orders in perturbation theory to give the running higgs mass. This technique is based on the fact that the Veltman functions [46] which appear in the diagrammatic method can be approximated by logarithms when there are two different scales in the problem. The RGE technique sums these logarithms to all orders, but drops all non–logarithmic, finite terms. These terms are often very important [34, 36]. Moreover, the reliability of the RGE treatment of the logarithmic terms decreases if the two scales are not very far apart (as is the case here, where the two scales are the EW and SUSY breaking scales). Numerically, the higgs mass calculated with the RGE method can differ by 10 GeV or more compared to the diagramatic method, even if two–loop RGEs are used.

The renormalization group improvement (see our eq. (9)) we use in our work replaces the logarithmic part of the corrections obtained with the diagrammatic method by the resummed logarithmic corrections as obtained with the renormalization group technique. Our results therefore incorporate both the important finite corrections at the two-loop level and the resummed leading and next–to–leading logarithmic corrections.

The second popular technique is the effective potential method. In ref. [34] the effective potential method is compared with the diagramatic technique. Working in an on–shell scheme in both methods, it is shown that the two techniques reproduce the same answer when the tree level higgs mass is zero and when all supersymmetric particles are included in the effective potential. On the contrary, if the tree level higgs mass is non–zero, the effective potential answer has to be corrected using diagramatic methods. With these diagrammatic corrections, the two methods become indistinguishable.

The effective potential method is used in ref. [47]. There the $\overline{MS}$ renormalization scheme is also used and so the comparison with our on–shell diagramatic method is not simple. A non–trivial ambiguity for the choice of the arbitrary scale is present in this method. A further limitation in this calculation is the inclusion in the effective potential of only SM particles. Important log terms arising from susy particle loops are therefore absent. When the susy particles are ignored, the only connection with supersymmetry is in the boundary condition for λ at the scale M_{SUSY}. A partial compensation is made by including the threshold effects of susy particles in the form of step–functions. What would be a full Veltman's function in the diagramatic method is approximated in the effective potential method by a step function shift[48] in the boundary condition: $\lambda = \frac{1}{4}(g^2 + g'^2)\cos^2 2\beta + \Delta\lambda$.

In our diagramatic method these approximations are not present since the effects of the non–logarithmic terms are included in the full expressions of the Veltman's functions. For example, important non–logarithmic effects are included, such as the decreasing of the higgs mass when $\tan\beta \to \infty$, $\mu \sim 1$ TeV and $A = 0$, as explained above and seen in Fig. 1. Also, the effect of large splitting in the masses of the stop squarks is automatically taken into

account in our diagramatic method. These effects are not included in ref. [47].

There are two further improvements that we have achieved. The first improvement is the use of different RGEs above and below the top quark mass. Below m_t the top quark mass decouples and the RGE for λ does not contain the top Yukawa coupling. This effect can be important. In principle, the RGE for the gauge couplings should also be modified. In practice, it is a negligible effect. (This modification is more complicated, since the electroweak gauge symmetry is broken. A careful analysis can be found in ref. [38].) The second improvement is the consideration of the running of $\tan\beta$. In practice, this effect is numerically small[38].

We finish this section with some comments on the decay $b \to s\gamma$. It is known that the branching ratio $B(b \to s\gamma)$ has a strong dependence on the susy higgs parameters [49, 50, 51]. However, when all squarks are heavy, as here, the contribution from the chargino/squark loops to $B(b \to s\gamma)$ is suppressed. In the case of heavy squarks, the charged–higgs/top–quark loop may seriously alter the rate, and strong constraints on the charged higgs minimum mass result [52, 51]. This constraint does not affect the present work, where we take m_A and therefore $m_{H^\pm}$ and m_H large in order to establish the light higgs upper bound: in the large m_A, large squark mass limit, the ratio $B(b \to s\gamma)$ approaches the SM value, consistent with the CLEO bound [53].

4 The lightest higgs in non-standard susy models

The MSSM can be extended in a straightforward fashion by adding an $SU(2)$ singlet S with vanishing hypercharge to the theory [54]. As a consequence, the particle spectrum contains an additional scalar, pseudoscalar, and neutralino. This extended model, the so–called (M+1)SSM, features four possible additional terms in the superpotential. Two of these terms, $\lambda S H_B \epsilon H_T$ and $\frac{1}{3}\kappa S^3$, enter into the calculation of the lightest higgs mass; λ enters directly, while κ enters through the RG equations. ϵ is the usual antisymmetric 2 by 2 matrix.

At tree-level, a study of the eigenvalues of the scalar mass matrix gives an upperbound on the mass of the lightest higgs boson:

$$m_h^2 \leq M_Z^2 \left\{ \cos^2 2\beta + 2\frac{\lambda^2}{g_1^2 + g_2^2} \sin^2 2\beta \right\}. \tag{10}$$

The first term on the right hand side is just the MSSM result of Eq. (6). The second term gives a positive contribution, and since the parameter λ is *a priori* free, weakens the upperbound considerably [55, 56]. However, there are two scenarios in which the bound prooves to be very restrictive. In the first scenario $\tan\beta$ is large, and therefore $\cos^2 2\beta$ is necessarily $\gg \sin^2 2\beta$. In the second scenario the value of λ is limited by the assumption of perturbative unification. In this latter scenario, even if λ assumes a high value at the GUT scale, the renormalization group equations drive the evolving value of λ to a moderate value at the SUSY breaking scale. The exact higgs mass upper bound depends on the value of the top yukawa g_t at the GUT scale through the renormalization group equations. Above M_{SUSY} the running of the coupling constants is described by the (M+1)SSM renormalization group

equations, whereas below this scale the SM renormalization group equations are valid. At M_{SUSY} the boundary conditions

$$\begin{aligned} \lambda^{SM} &= \frac{1}{8}\left(g_1^2+g_2^2\right)\left(\cos^2 2\beta + 2\frac{\lambda^2}{g_1^2+g_2^2}\sin^2 2\beta\right), \\ g_t^{SM} &= g_t \sin\beta, \end{aligned} \tag{11}$$

incorporate the transition from the (M+1)SSM to the SM. Here λ^{SM} and g_t^{SM} are the standard model higgs self–coupling and top quark yukawa coupling respectively. The value of the higgs boson mass is determined implicitly by the equation $2\lambda^{SM}(m_h)\, v_{SM}^2 = m_h^2$. This RGE procedure of running couplings from M_{SUSY} down to the weak scale takes into account logarithmic radiative corrections to the higgs boson mass, including in particular those caused by the heavy top quark.

In Fig. 2 we show the maximum value of the higgs boson mass as a function of $\tan\beta$ for the chosen values of the top quark mass m_t. We have adopted a susy–breaking scale of $M_{SUSY} = 1\ TeV$; this value is consistent with the notion of stabilizing the weak–to–susy GUT hierarchy, and is the value favored by RGE analyses of the observables $\sin^2\theta_W$ and m_b/m_τ. The bounds in Fig. 2 are quite insensitive to the choice of M_{SUSY}, increasing very slowly as M_{SUSY} increases [55]. We have assumed that all superpartners and all higgs bosons except for the lightest one are heavy, i. e. $\sim M_{SUSY}$. For low values of the top quark mass ($\sim M_Z$), the mass upper bound on the higgs boson in the (M+1)SSM will be substantially higher than in the MSSM at $\tan\beta \lesssim$ a few. This is because $\lambda(m_h)$ is large for low m_t, and because $\sin^2 2\beta \gtrsim \cos^2 2\beta$ for $\tan\beta \lesssim$ a few. However, for a larger top quark mass, as in Fig. 2, the difference between the MSSM and (M+1)SSM upper bounds diminishes. This is because $\lambda(m_h)$ falls with increasing m_t, and because there is an increasing minimum value for $\sin\beta = g_t^{SM}/g_t$ [from the second of Eqs. (11)], and therefore for $\tan\beta$, when $m_t \propto g_t^{SM}$ is raised and g_t is held to be perturbatively small up to the GUT scale[8]. This increasing minimum value of $\tan\beta$ is evident in the curves of Fig. 2. A comparison of Figs. 1 and 2 reveals that the (M+1)SSM and MSSM bounds are very similar at $\tan\beta \gtrsim 6$. For m_t at or above the CDF value, only this $\tan\beta \gtrsim 6$ region is viable in the (M+1)SSM model.

In a fashion very similar to the (M+1)SSM, perturbative unificaton yields a bound on the mass of the lightest higgs bosons in more complicated extensions of the MSSM. In general, the lowest eigenvalue of the scalar mass matrix is bounded by M_Z times a factor which depends on the dimensionless coupling constants in the higgs sector. The renormalizaton group equations force these coupling constants to assume relatively low values at the SUSY breaking scale, and as a consequence the mass bound on the lightest higgs boson is of the order of M_Z.

Although a bound on the mass of the lightest higgs boson exists in perturbative SUSY models, this is not the case in SUSY models with a strongly interacting symmetry breaking sector. The low energy physics of this class of theories is described by a supersymmetric non-linear sigma model, which is obtained by imposing the constraint $H_T \epsilon H_B = \frac{1}{4} v_{SM}^2 \sin^2 2\beta$ on the action of the MSSM [57]. This constraint is the only one possible in the MSSM

[8]Keeping g_t perturbatively small up to the GUT scale implies $m_t \leq$ its pseudo fixed–point value of $\sim 200 \sin\beta$. Therefore, a measured top mass as large as that reported by CDF requires $\tan\beta > 1$ in the GUT scenario, and suggests saturation of the fixed–point.

higgs sector that obeys supersymmetry, is invariant under $SU(2) \times U(1)$, and leaves the vev in a global minimum [9]. As a result of this constraint one of the scalar higgs bosons, the pseudoscalar, and one of the neutralinos are eliminated from the particle spectrum. The remaining higgs boson has a mass $m_h^2 = M_Z^2 + (\hat{m}_T^2 + \hat{m}_B^2) \sin^2 2\beta$, and the charged higgs bosons have masses $m_{H^\pm}^2 = M_W^2 + (\hat{m}_T^2 + \hat{m}_B^2)$. Here, $\hat{m}_T^2$ and $\hat{m}_B^2$ are soft, dimensionful, susy–breaking terms; they may be positive or negative.

In order for the notion of a supersymmetric non-linear model to be relevant, the susy breaking scale is required to be much smaller than the chiral symmetry breaking scale $4\pi v_{SM}$. The natural magnitude for the parameters $\hat{m}_B^2$ and $\hat{m}_T^2$ is therefore of the order of M_Z^2. Consequently, both the neutral and the charged higgs bosons have masses of at most a few multiples of M_Z in the non–linear model. This formalism of the effective action allows a description of the low energy physics *independent* of the particular strongly–interacting underlying theory from which it derives. Thus we believe that the non–linear MSSM model presented here is probably representative of a class of underlying strongly–interacting susy models. The lesson learned then is that measuring a value for m_h at $\lesssim 300$ GeV cannot validate the SM, MSSM, (M+1)SSM, or any other electroweak model. However, the premise of this present article remains valid, that such a measurement should rule out one or more of these popular models.

5 Supersymmetric Grand Unified Theories

Supersymmetric grand–unified theories (susy GUTs) are the only simple models in which the three low energy gauge coupling constants are known to merge at the GUT scale, and hierarchy and parameter–naturalness issues are solved. Thus, it is well motivated to consider the grand unification of the low energy susy models. At low energies, SUSY GUT models reduce to the MSSM, but there are additional relations between the parameters [42]. The additional constraints must yield an effective low energy theory that is a special case of the general MSSM we have just considered. Therefore, the upper bound [10] on m_h in such SUSY GUT models is in general *lower* than in the MSSM without any restrictions. The assumption of gauge coupling constant unification (with its implied desert between M_{SUSY} and M_{GUT}) presents no significant constraints on the low energy MSSM parameters [42, 58]. However, the further assumption that the top yukawa coupling remains perturbatively small up to M_{GUT} leads to the low energy constraint $0.96 \leq \tan\beta$. This is because the RGE evolves a large but perturbative top yukawa coupling at M_{GUT} down to its well–known infrared pseudo–fixed–point value at M_{SUSY} and below, resulting in the top mass value $\sim 200 \sin\beta$ GeV. If the bottom yukawa is also required to remain perturbatively small up to M_{GUT}, then $\tan\beta \leq 52$ [59] emerges as a second low energy constraint.

The pseudo–fixed–point solution is not a true fixed–point, but rather is the low energy

[9] This MSSM non–linear sigma model is not the formal heavy higgs limit of the MSSM, but is a heavy higgs limit of the (M+1)SSM; the MSSM does not contain an independent, dimensionless, quartic coupling constant λ in the higgs sector which can be taken to infinity, whereas the (M+1)SSM (and the SM) does.

[10] In fact, the additional restrictions may be so constraining as to also yield a *lower* limit on the lightest higgs mass, in addition to the upper limit. For example, $m_h > 85$ GeV for $\tan\beta > 5$ and $m_t = 170$ GeV is reported in ref.[42], and a similar result is given in [43].

yukawa value that runs to become a Landau pole (an extrapolated singularity, presumably tamed by new physics) near the GUT scale. The apparent CDF top mass value is within the estimated range of the pseudo–fixed–point value. Thus it is attractive to assume the pseudo–fixed–point solution. With the additional assumptions that the electroweak symmetry is radiatively broken [60] (for which the magnitude of the top mass is crucial) and that the low energy MSSM spectrum is defined by a small number of parameters at the GUT scale (the susy higgs mass parameter μ – which is also the higgsino mass, and four universal soft susy–breaking mass parameters: the scalar mass, the bilinear and trilinear masses, and the gaugino mass), two compact, disparate ranges for $\tan\beta$ emerge: $1.0 \leq \tan\beta \leq 1.4$ [59], and a large $\tan\beta$ solution $\sim m_t/m_b$. [11] Reference to our Figs. 1 and 2 shows that the gap between the SM and MSSM is maximized in the small $\tan\beta$ region and minimized in the large $\tan\beta$ region, whereas just the opposite is true for the gap between the SM and (M+1)SSM models. Moreover, the (M+1)SSM model is an inconsistent theory in the small $\tan\beta$ region if $m_t \gtrsim 160$ GeV.

In fact, a highly constrained low $\tan\beta$ region ~ 1 and high $\tan\beta$ region $\gtrsim$ 40–70 also emerge when bottom–τ yukawa unification at the GUT scale is imposed on the radiatively broken model [61, 62, 63, 64]. Bottom–τ yukawa coupling unification is attractive in that it is natural in susy SU(5), SO(10), and E_6, and explains the low energy relation, $m_b \sim 3m_\tau$. With bottom-τ unification, the low to moderate $\tan\beta$ region requires the proximity of the top mass to its fixed–point value [65], while the high $\tan\beta$ region also requires the proximity of the bottom and τ yukawas to their fixed–point; the emergence of the two $\tan\beta$ regions results from these two possible ways of assigning fixed–points.

The net effect of the yukawa–unification constraint in susy GUTs is necessarily to widen the mass gap between the light higgs MSSM and the heavier higgs SM, thus strengthening the potential for experiment to distinguish the models. The large $\tan\beta$ region is disfavored by proton stability [66]. Adoption of the favored low to moderate $\tan\beta$ region leads to a highly predictive framework for the higgs and susy particle spectrum [63, 64]. In particular, the fixed–point relation $\sin\beta \sim m_t/(200GeV)$ fixes $\tan\beta$ as a function of m_t. For a heavy top mass as reported by CDF, one has $\tan\beta \sim$ (1, 2) for $m_t =$ (140, 180) GeV. Since $\tan\beta \sim 1$ is the value for which the m_h upper bound is minimized (the tree–level contribution to m_h vanishes), the top yukawa fixed–point models offer a high likelihood for h^0 detection at LEP200. Reduced m_h upper bounds have been reported in [62, 63]. The reduction in these bounds is due to the small $\tan\beta$ restriction, an inevitable consequence of assigning the top mass, but not the bottom mass, to the pseudo fixed–point. These bounds are basically our bound in Fig. 1 for $\tan\beta \sim 1$, when allowance is made for small differences resulting from different methods and approximations.

Even more restrictive susy GUTs have been analyzed. These include the "no–scale" or minimal supergravity models [67], in which the soft mass parameters m_0 (universal scalar mass) and A are zero at the GUT scale; and its near relative, the superstring GUT, in which the dilaton vev provides the dominant source of susy breaking and so m_0, A, and the gaugino mass parameter all scale together at the GUT scale [68]. Each additional constraint serves to further widen the SM/MSSM higgs mass gap.

[11] It may be noteworthy that a fit of MSSM radiative corrections to the electroweak datum $R_b \equiv \Gamma(Z \to b\bar{b})/\Gamma(Z \to hadrons)$ reveals a preference for just these two $\tan\beta$ regions [45].

In radiatively broken susy GUTs with universal soft parameters, the superparticle spectrum emerges at $\lesssim 1$ TeV. If the spectrum in fact saturates the 1 TeV value, then as we have seen the Feynman rules connecting h^0 to SM particles are indistinguishable from the Feynman rules of the SM higgs. Thus, it appears that if a susy GUT is the choice of Nature, then the mass of the lightest higgs, but not the higgs production rate or dominant higgs decay modes, may provide our first hint of grand unification.

6 Discovery potential for the higgs boson

The higgs discovery potential of LEPII [69, 70] depends on the energy at which the machine is run. A SM higgs mass up to 105 GeV is detectable at LEPII with the $\sqrt{s} = 200$ GeV option (LEP200), while a SM higgs mass only up to 80 GeV is detectable with LEP178. As we have shown, with the large value of m_t reported by CDF, the upper limit on the MSSM h^0 mass is ~ 120 GeV. This limit is ~ 10 GeV lower than that reported in our previous work[5], as a result of the inclusion of RGE–resummed leading and next-to leading logarithms and 2–loop finite QCD corrections. Near this upper limit the MSSM higgs has the production and decay properties of the SM higgs. Discovery of this lightest MSSM higgs then argues strongly for the LEP200 option over LEP178. Furthermore, for any choices of the MSSM parameters, associated production of either $h^0 Z$ or $h^0 A$ is guaranteed at LEP200 as long as $m_{\tilde{t}} \lesssim 300$ GeV [69]. Even better would be LEP230, where detection of Zh^0 is guaranteed as long as $m_{\tilde{t}} \lesssim 1$ TeV [69]. At an NLC300 (the Next Linear Collider), detection of Zh^0 is guaranteed for MSSM or for (M+1)SSM [69]. Turning to hadron colliders [71, 72], it is now believed that while the SM higgs cannot be discovered at Fermilab's Tevatron with its present energy and luminosity, the mass range 80 GeV to 130 GeV is detectable at any hadron collider with $\sqrt{s} \gtrsim 2$ TeV and an integrated luminosity $\int dt\, \mathcal{L} \gtrsim 10\text{fb}^{-1}$ [72]; the observable mass window widens significantly with increasing luminosity, but very little with increasing energy. For brevity, we will refer to this High Luminosity DiTevatron hadron machine as the "HLDT". If the SM desert ends not too far above the electroweak scale, then the SM higgs may be as heavy as $\sim$ 600–800 GeV [12] (but not heavier, according to the triviality argument), in which case only the LHC (and not even the NLC500) guarantees detection.

We present our conclusions on detectability for the CDF central m_t value, for the $m_t \pm 1\sigma$ values, and for a $m_t - 3\sigma$ value of 137 GeV:
(i) if $m_t \sim 137$ GeV, the SM higgs mass lower bound from absolute vacuum stability is equal to the experimental lower bound of $m_H = 64$ GeV, while the metastability bound allows a mass as low as 43 GeV [13]; a SM mass up to (80, 105, 130) GeV is detectable at (LEP178, LEP200, HLDT); and the MSSM h^0 is certainly detectable at LEP178 for $\tan\beta \sim$ 1–2, and certainly detectable at LEP200 for all $\tan\beta$.
(ii) if $m_t \sim 163$ GeV, then the abolute (metastability) SM lower bound rises to 109 (96) GeV, so the SM higgs cannot be detected at LEP178 and probably not at LEP200, but is still detectable at the HLDT if its mass is below 130 GeV; the lightest MSSM higgs is certainly detectable at LEP178 if $\tan\beta$ is very close to 1, and is certainly detectable at LEP200 if

[12] Theorists would prefer an even lower value of $\lesssim 400$ GeV, so that perturbative calculations in the SM converge [73].

[13] Recall that for the SM vacuum stability and metastability bounds we assume a desert up to $\sim 10^{10}$ GeV.

$\tan\beta$ is $\lesssim 3$.
(iii) if $m_t \sim 176$ GeV, then the SM higgs is above 131 (123) GeV, out of reach for LEPII and probably the HLDT as well; the MSSM higgs is certainly detectable at LEP200 if $\tan\beta \sim$ 1–2.
(iv) if $m_t \sim 189$ GeV, then the SM higgs is above 153 (150) GeV in mass; at any $\tan\beta$ value, the MSSM higgs is not guaranteed to be detectable at LEP200, but is certainly detectable at the HLDT if $\tan\beta \sim$ 1–3.
For these mass bounds the value $\alpha_s = 0.118$ has been assumed. The MSSM mass upper bound is relatively insensitive to changes in α_s, whereas the SM mass lower bounds decrease about 3 GeV with each 0.005 increase in α_s. It is interesting that the h^0 mass range is most accessible to experiment is $\tan\beta \sim$ 1–3, just the parameter range favored by susy GUTs.

7 Discussion and conclusions

For a top quark mass ~ 176 GeV, the central value reported by CDF, and an α_s value of ~ 0.118, a measurement of the mass of the higgs boson will distinguish the SM with a $\gtrsim 10^{10}$ GeV desert from the MSSM with a SUSY breaking scale of about 1 TeV. For the (M+1)SSM with the assumption of perturbative unification, conclusions are similar to those of the MSSM. For α_s above 0.120 and $m_t \sim 176$ GeV, a small overlap of the SM and MSSM mass regions exists, but it is a priori unlikely that the higgs mass will be found in this small range. Accordingly, the first higgs mass measurement can be expected to eliminate one of these popular models.

Most of the range of the lightest MSSM higgs mass is accessible to LEPII. The lightest MSSM higgs is guaranteed detectable at LEP230 and at the LHC; and the lightest (M+1)SSM higgs is guaranteed detectable at a NLC300 and at the LHC. Since there is no lower bound on the lightest MSSM higgs mass other than the experimental bound, the MSSM h^0 is possibly detectable even at LEP178 for all $\tan\beta$, but there is no guarantee. In contrast, the SM higgs is guaranteed detectable only at the LHC; if $m_t \sim 176$ GeV, then according to the vacuum stability (metastability) argument, the SM higgs mass exceeds 131 (123) GeV, and so likely will not be produced until the LHC or NLC is available.

Thus, one simple conclusion is that LEPII has a tremendous potential to distinguish MSSM and (M+1)SSM symmetry breaking from SM symmetry breaking. If a higgs is discovered at LEPII, the higgs sector of the SM with a large desert is ruled out.

Acknowledgements:
This work was supported in part by the U.S. Department of Energy grant no. DE-FG05-85ER40226, and the Texas National Research Laboratory Commission grant no. RGFY93–303.

References

[1] The LEP Electroweak Working Group (Aleph, Delphi, L3, Opal), CERN preprint PPE/93–157 (1993).

[2] J. Ellis, G. L. Fogli, and E. Lisi, preprint CERN–TH/95–202.

[3] F. Abe et al. CDF Collaboration, *Phys. Rev. Lett.* **74**, 2626 (1995); *Phys. Rev.* **D52**, R2605 (1995).

[4] N. V. Krasnikov and S. Pokorski, *Phys. Lett. B* **288**, 184 (1992).

[5] Marco A. Díaz, Tonnis A. ter Veldhuis, and Thomas J. Weiler, *Phys. Rev. Lett* **74**, 2876 (1995).

[6] J.A. Casas, J.R. Espinosa, and M. Quirós, *Phys. Lett. B* **342**, 171 (1995).

[7] M. A. Díaz, preprint VAND–TH–94–16, SHEP–95–38, in progress.

[8] M.A. Díaz, preprint VAND–TH–94–19 (hep-ph-9408320), presented at 1994 Meeting of the APS, DPF'94, Albuquerque, New Mexico, 2-6 Aug. 1994.

[9] G. Altarelli and G. Isidori, *Phys. Lett. B* **337**, 141 (1994).

[10] J. R. Espinosa and M. Quiros, *Phys. Lett.* **B353**, 257 (1995).

[11] H. Haber, Proc. of the "Workshop on Physics from the Planck Scale to the Electroweak Scale," Univ. Warsaw, Poland, September 1994, and preprint SCIPP 94/39 (hep–ph 9501320).

[12] *The Higgs Hunter's Guide*, J. F. Gunion, H. E. Haber, G. L. Kane, and S. Dawson, Addison-Wesley, Redwood City, CA (1990).

[13] P. H. Chankowski, S. Pokorski, and J. Rosiek, *Phys. Lett. B* **281**, 100 (1992); and in the context of susy GUTs, refs. [42, 43].

[14] H.E. Haber and R. Hempfling, *Phys. Rev. Lett.* **66**, 1815 (1991); Y. Okada, M. Yamaguchi and T. Yanagida, *Prog. Theor. Phys.* **85**, 1 (1991); J. Ellis, G. Ridolfi and F. Zwirner, *Phys. Lett. B* **257**, 83 (1991).

[15] R. Dashen and H. Neuberger, *Phys. Rev. Lett.* **50** 1897 (1983); M.A.B. Beg, C. Panagiotakopoulos and A. Sirlin, *Phys. Rev. Lett.* **52** 833 (1984).

[16] Non-perturbative lattice results are obtained in J. Kuti, L. Lin and Y. Shen, *Phys. Rev. Lett.* **61** 678 (1988); M. Lüscher and P. Weisz, *Nucl. Phys.* **B318** 705 (1989); G. Bhanot, K. Bitar, U. Heller and H. Neuberger, *Nucl. Phys.* **B353** 551 (1991).

[17] Non-perturbative Wilson RGE results are obtained in P. Hasenfratz and J. Nager, *Z. Phys.* **C37** 477 (1988); R. Akhoury and B. Haeri, *Phys. Rev. D* **48** 1252 (1993). T.E. Clark, B. Haeri and S.T. Love, *Nucl. Phys.* **B402** 628 (1993); T.E. Clark, B. Haeri, S.T. Love, W.T.A. ter Veldhuis and M.A. Walker, *Phys. Rev. D* **50** 606 (1994).

[18] M. Lindner, M. Sher, and H. W. Zaglauer, *Phys. Lett. B* **228**, 139 (1989); U. Ellwanger and M. Lindner, *Phys. Lett. B* **301**, 365 (1993).

[19] See, e. g. M. Lindner, *Z. Phys.* **C31**, 295 (1986).

[20] Two excellent reviews of the effective potential physics and bounds are: M. Sher, *Phys. Rep.* **179**, 273 (1989); and H. E. Haber, *Lectures on Electroweak Symmetry Breaking*, TASI, Boulder, CO (1990).

[21] A. Linde, *Phys. Lett. B* **62**, 435 (1976); S. Weinberg, *Phys. Rev. Lett.* **36**, 294 (1976).

[22] F. Abe et al., CDF Collaboration, *Phys. Rev. Lett.* **73**, 220 (1994).

[23] S. Abachi at al. *Phys. Rev. Lett.* **74**, 2632 (1995).

[24] P. Arnold and M. Vokos, *Phys. Rev. D* **44**, 3620 (1991); G. W. Anderson, *Phys. Lett. B* **243**, 265 (1990).

[25] D. Buskulic et al., the ALEPH Collaboration, *Phys. Lett. B* **313**, 312 (1993) establish a 62 GeV lower bound; a 64 GeV lower bound has been reported by J. Schwidling, Proc. of the Int. Europhysics Conference, Marseille, France, July 1993.

[26] Particle Data Group, Review of Particle Properties, p. 1302, *Phys. Rev.* **D50**, 1173 (1994).

[27] P. H. Chankowski and S. Pokorski, update (hep–ph/9509207) to *Phys. Lett.* **B356**, 307 (1995).

[28] J. Bjorken, *Phys. Rev.* **148**, 1467 (1966); **D1**, 1376 (1970).

[29] J. Ellis and M. Karliner, hep–ph/9510402.

[30] The LEP collaborations, ALEPH, DELPHI, L3, OPAL, and the LEP Electroweak Working Group, CERN/PPE/93–157, August 1993.

[31] M. Sher, *Phys. Lett. B* **317**, 159 (1993), and Addendum (1994) hep-ph #9404347; see also C. Ford, D. R. T. Jones, P. W. Stevenson and M. B. Einhorn, *Nucl. Phys.* **B395**, 62 (1993).

[32] M.S. Berger, *Phys. Rev. D* **41**, 225 (1990); R. Barbieri, M. Frigeni, F. Caravaglios, *Phys. Lett. B* **258**, 167 (1991); R. Barbieri and M. Frigeni, *Phys. Lett. B* **258**, 395 (1991); Y. Okada, M. Yamaguchi and T. Yanagida, *Phys. Lett. B* **262**, 54 (1991); A. Yamada, *Phys. Lett. B* **263**, 233 (1991); J. Ellis, G. Ridolfi and F. Zwirner, *Phys.Lett. B* **262**, 477 (1991); A. Brignole, *Phys. Lett. B* **281**, 284 (1992).

[33] M. Drees and M.M. Nojiri, *Phys. Rev. D* **45**, 2482 (1992).

[34] M.A. Díaz and H.E. Haber, *Phys. Rev. D* **46**, 3086 (1992).

[35] J.F. Gunion and A. Turski, *Phys. Rev. D* **39**, 2701 (1989); **40**, 2333 (1989); A. Brignole, J. Ellis, G. Ridolfi, and F. Zwirner, *Phys. Lett. B* **271**, 123 (1991); A. Brignole, *Phys. Lett. B* **277**, 313 (1992); P.H. Chankowski, S. Pokorski, and J. Rosiek, *Phys. Lett. B* **274**, 191 (1992).

[36] M.A. Díaz and H.E. Haber, *Phys. Rev. D* **45**, 4246 (1992).

[37] P. H. Chankowski, S. Pokorski and J. Rosiek, *Nucl. Phys.* **B423**, 437 (1994).

[38] H.E. Haber and R. Hempfling, *Phys. Rev. D* **48**, 4280 (1993).

[39] R. Hempfling and A. H. Hoang, *Phys. Lett. B* **331**, 99 (1994).

[40] J. R. Espinosa and M. Quirós, *Phys. Lett. B* **266**, 389 (1991).

[41] P. Langacker and M. Luo, *Phys. Rev. D* **44**, 817 (1991); U. Amaldi, W. de Boer, and H. Furstenau, *Phys. Lett. B* **260**, 447 (1991).

[42] G. L. Kane, C. Kolda, L. Roszkowski, and J. D. Wells, *Phys. Rev. D* **49**, 6173 (1994), and references therein.

[43] J. Lopez, D. V. Nanopoulos, H. Pois, X. Wang, and A. Zichichi, *Phys. Lett. B* **306**, 73 (1993).

[44] B. de Carlos and J.A. Casas, *Phys. Lett. B* **309**, 320 (1993).

[45] P. H. Chankowski and S. Pokorski, preprint hep–ph/9505308; S. Pokorski, preprint hep–ph/9510224.

[46] G.'t Hooft and M. Veltman, *Nucl. Phys.* **B153**, 365 (1979); G. Passarino and M. Veltman, *Nucl. Phys.* **B160**, 151 (1979).

[47] J.A. Casas, J.R. Espinosa, M. Quirós, and A. Riotto, *Nucl. Phys.* **B436**, 3 (1995), Erratum *Nucl. Phys.* **B439**, 466 (1995).

[48] R. Hempfling, preprint DESY-93-012, Feb. 1993.

[49] S. Bertolini, F. Borzumati, A. Masiero, and G. Ridolfi, *Nucl. Phys.* **B353**, 591 (1991); N. Oshimo, *Nucl. Phys.* **B404**, 20 (1993); J.L. Lopez, D.V. Nanopoulos, and G.T. Park, *Phys. Rev. D* **48**, 974 (1993); Y. Okada, *Phys. Lett. B* **315**, 119 (1993); R. Garisto and J.N. Ng, *Phys. Lett. B* **315**, 372 (1993); J.L. Lopez, D.V. Nanopoulos, G.T. Park, and A. Zichichi, *Phys. Rev. D* **49**, 355 (1994); M.A. Díaz, *Phys. Lett. B* **322**, 207 (1994); F.M. Borzumati, *Z. Phys.* **C63**, 291 (1994); S. Bertolini and F. Vissani, *Z. Phys.* **C67**, 513 (1995).

[50] B. de Carlos and J.A. Casas, *Phys. Lett. B* **349**, 300 (1995).

[51] M.A. Díaz, *Phys. Lett. B* **304**, 278 (1993).

[52] J.L. Hewett, *Phys. Rev. Lett.* **70**, 1045 (1993); V. Barger, M.S. Berger and R.J.N. Phillips, *Phys. Rev. Lett.* **70**, 1368 (1993).

[53] R. Ammar et al. (CLEO Collaboration), *Phys. Rev. Lett.* **71**, 674 (1993); M. S. Alam et al. (CLEO Collaboration), *Phys. Rev. Lett.* **74**, 2885 (1995).

[54] J. Ellis, J.F. Gunion, H.E. Haber, L. Roszkowski and F. Zwirner, *Phys. Rev. D* **39**, 844 (1989); M. Drees, *Int. J. Mod. Phys.* **A4**, 3635 (1989).

[55] W.T.A. ter Veldhuis, Purdue Preprint PURD-TH-92-11.

[56] P. Binetruy and C. A. Savoy, *Phys. Lett. B* **277**, 453 (1992); G.L. Kane, C. Kolda and J.D. Wells, *Phys. Rev. Lett.* **70** 2686 (1993); J.R. Espinosa and M. Quirós, *Phys. Lett. B* **302** 51 (1993); D. Comelli and E. Verzegnassi, *Phys. Rev. D* **47** 764 (1993); T. Elliot, S.F. King and P.L. White, *Phys. Lett. B* **305**, 71 (1993); P.N. Pandita, *Phys. Lett. B* **318**, 338 (1993).

[57] S. Ferrara, A. Masiero and M.Poratti, *Phys. Lett. B* **301** (1993) 358; S. Gerrara and A. Masiero, CERN preprint CERN TH-6846-93, to appear in the Proceedings of SUSY 93, World Scientific, ed. by P. Nath; S. Ferrara, A. Masiero, M. Porrati and R. Stora, *Nucl.Phys.* **B417**, 238 (1994); T.E. Clark and W.T.A. ter Veldhuis, *Nucl. Phys.* **B426**, 385 (1994); W.T.A. ter Veldhuis, *Mod. Phys. Lett.* **A9**, 3691 (1994); K.J. Barnes, D.A. Ross and R.D. Simmons, *Phys. Lett. B* **338**, 457 (1994).

[58] P. Langacker and N. Polonsky, *Phys. Rev. D* **47**, 4028 (1993).

[59] V. A. Bednyakov, W. de Boer, and S. G. Kovalenko, preprint hep–ph #9406419, June 1994.

[60] M. Drees and M. Nojiri, *Nucl. Phys.* **B369**, 54 (1992).

[61] H. Arason et al. *Phys. Rev. Lett.* **67**, 29 (1991), and *Phys. Rev. D* **46**, 3945 (1992); D. J. Castano, E. J. Piard and P. Ramond, *Phys. Rev. D* **49**, 4882 (1994); M. Carena, T. E. Clark, C. E. M. Wagner, W. A. Bardeen and K. Sasaki, *Nucl. Phys.* **B369**, 33 (1992).

[62] V. Barger, M. S. Berger, P. Ohmann, and R. J. N. Phillips, *Phys. Lett. B* **314**, 351 (1993); M. Carena and C. E. M. Wagner, CERN–TH.7320/94, to appear in the Proc. of the "2nd IFT Workshop on Yukawa Couplings and the Origins of Mass", Gainesville, FL, Feb. 1994, and references therein.

[63] P. Langacker and N. Polonsky, *Phys. Rev. D* **49**, 1454 (1994); **50**, 2199 (1994); N. Polonsky, U. Penn preprint UPR–0595T, presented at SUSY–94, Ann Arbor MI, May 14–17, 1994; C. Kolda, L. Roszkowski, J. D. Wells, and G. L. Kane, *Phys. Rev. D* **50**, 3498 (1994), and references therein.

[64] M. Carena, M. Olechowski, S. Pokorski, and C. E. M. Wagner, *Nucl. Phys.* **B419**, 213 (1994).

[65] W. A. Bardeen, M. Carena, S. Pokorski, and C. E. M. Wagner, *Phys. Lett. B* **320**, 110 (1994).

[66] R. Arnowitt and P. Nath, *Phys. Rev. Lett.* **69**, 1014 (1992); *Phys. Lett. B* **287**, 89 (1992), and **289**, 368 (1992).

[67] S. Kelley, J. Lopez, D. Nanopoulos, H. Pois, and K. Yuan, *Phys. Lett. B* **285**, 61 (1992); R. Arnowitt and P. Nath, *Phys. Lett. B* 289, 368 (1992); J. Lopez, D. Nanopoulos, H. Pois, X. Wang, amd A. Zichichi, *Phys. Rev. D* **48**, 4062 (1993); J. F. Gunion and H. Pois, *Phys. Lett. B* **329**, 136 (1994).

[68] H. Baer, J. F. Gunion, C. Kao, and H. Pois, *Phys. Rev. D* **51**, 2159 (1995).

[69] J. F. Gunion, "Searching for the Higgs Boson(s)", to appear in Proc. of the Zeuthen Workshop — LEP200 and Beyond, Teupitz/Brandenburg, Germany, 10–15 April, 1994, eds. T Riemann and J Blumlein; and refs. therein.

[70] A. Djouadi, J. Kalinowski and P. M. Zerwas, *Z. Phys.* **C57**, 569 (1993); V. Barger, K. Cheung, A. Djouadi, B. A. Kniehl, and P. M. Zerwas, *Phys. Rev. D* **49**, 79 (1994); A. Djouadi, *Int. J. Mod. Phys.* **A10**, 1 (1995); and refs. therein.

[71] M. Spira, A. Djouadi, D. Graudenz, and P. M. Zerwas, *Phys. Lett. B* **318**, 347 (1993).

[72] S. Mrenna and G. L. Kane, Caltech preprint CIT 68–1938, and hep–ph #9406337.

[73] L. Durand, B. A. Kniehl and K. Riesselmann, *Phys. Rev. Lett.* **72**, 2534 (1994), have shown that the two loop contribution to higgs decay to $f\bar{f}$ exceeds the one loop contribution if the higgs mass exceeds ~ 400 GeV.

Figure Captions:

Fig. 1 The curves reveal the upper bound on the lightest MSSM higgs particle vs. $\tan\beta$, for top mass values of (a) 163 GeV, (b) 176 GeV, and (c) 189 GeV. Three extreme choices of susy parameters are invoked: the solid curve is for $\mu = A_t = A_b = 0$, the dashed curve is for $\mu = A_t = A_b = 1$ TeV, and the dot-dashed curve is for $\mu = -1$ TeV, $A_t = A_b = 1$ TeV. In all cases, $m_A = m_{\tilde{q}} = 1$ TeV and $m_b(M_Z) = 4$ GeV are assumed. The horizontal dotted lines are the ($\tan\beta$–independent) SM lower bounds on the higgs mass; the more restrictive stability bound derives from requiring that the EW vev sits in an absolute minimum, while the less restrictive metastability bound derives from requiring that the vev lifetime in the local EW minimum exceed the age of the universe.

Fig. 2

Upper bound on the lightest (M+1)SSM higgs vs. $\tan\beta$, for the top mass values (a) 163 GeV, (b) 176 GeV, and (c) 189 GeV. All superparticles and higgses beyond the lightest are assumed to be heavy, of order of the chosen susy–breaking scale of 1 TeV. The GUT scale is taken as 10^{16} GeV.

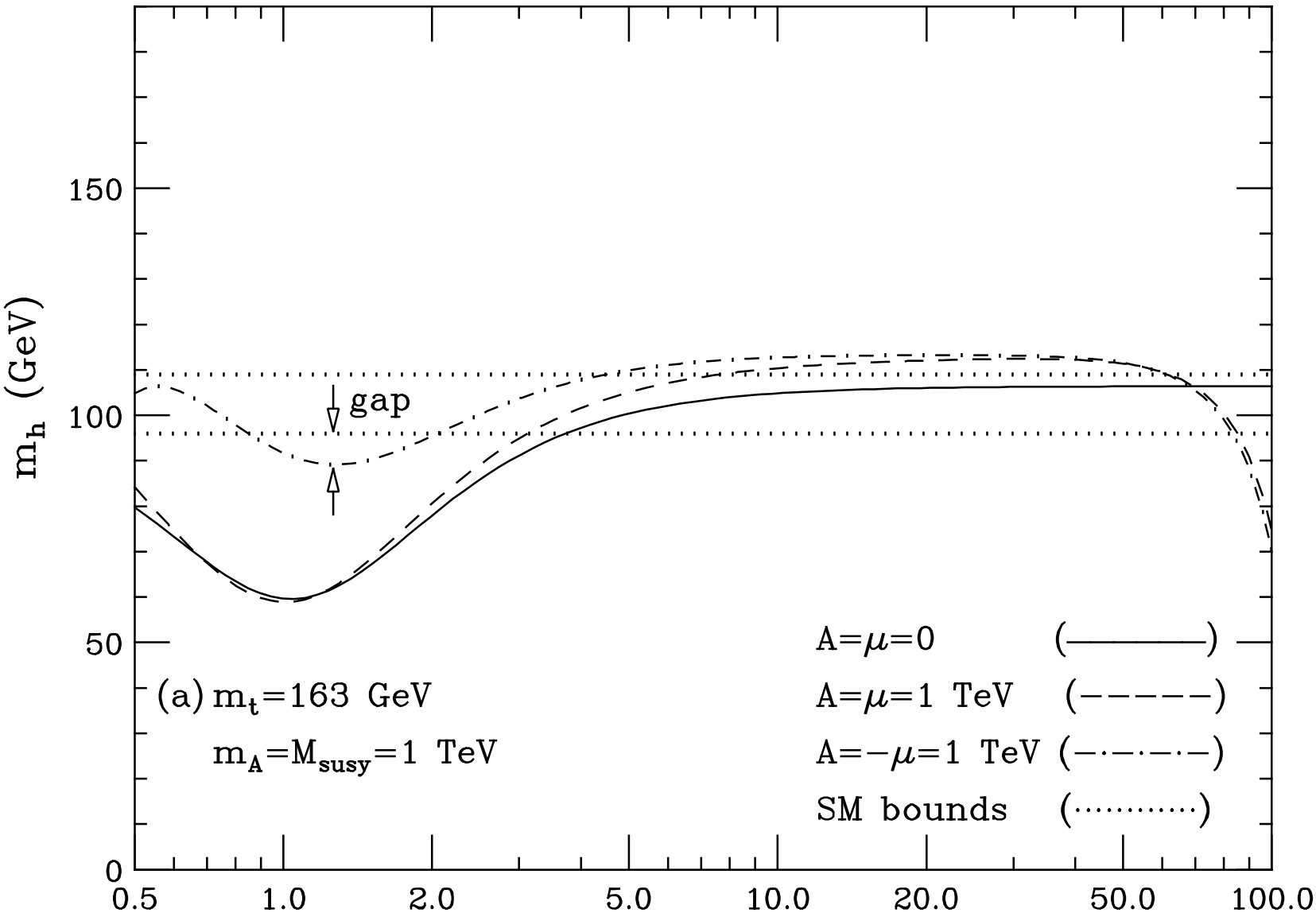
150
100
50
0
m_h (GeV)
gap
(a) m_t=163 GeV
m_A=M_{susy}=1 TeV
A=μ=0 (————)
A=μ=1 TeV (– – – – –)
A=−μ=1 TeV (–·–·–·–)
SM bounds (·····)
0.5
1.0
2.0
5.0
10.0
20.0
50.0
100.0
tan β

Fig. 1(a)

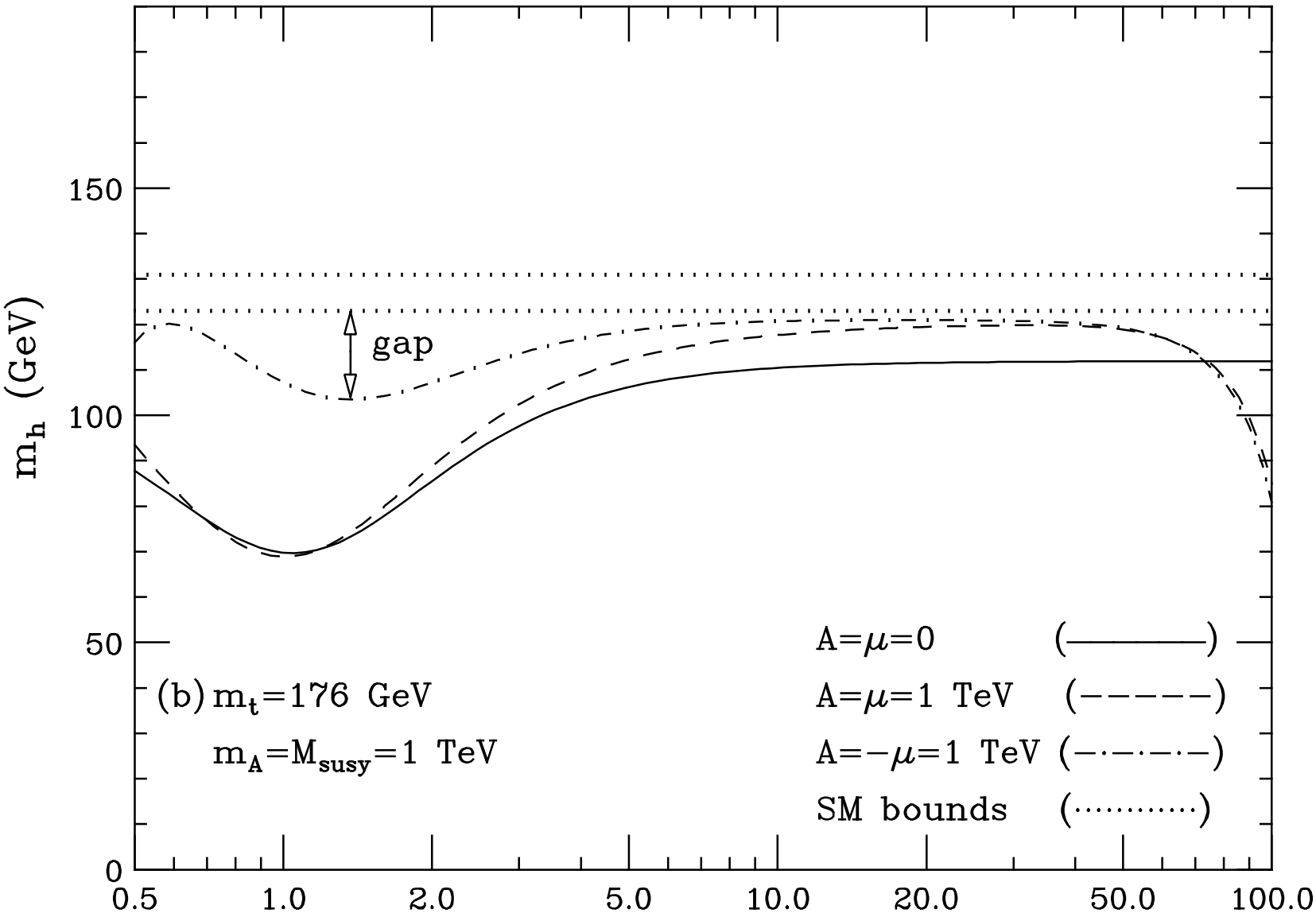
150
100
50
0
m_h (GeV)
gap
(b) m_t=176 GeV
m_A=M_{susy}=1 TeV
A=μ=0 (————)
A=μ=1 TeV (– – – – –)
A=−μ=1 TeV (–·–·–·–)
SM bounds (·····)
0.5
1.0
2.0
5.0
10.0
20.0
50.0
100.0
tan β

Fig. 1(b)

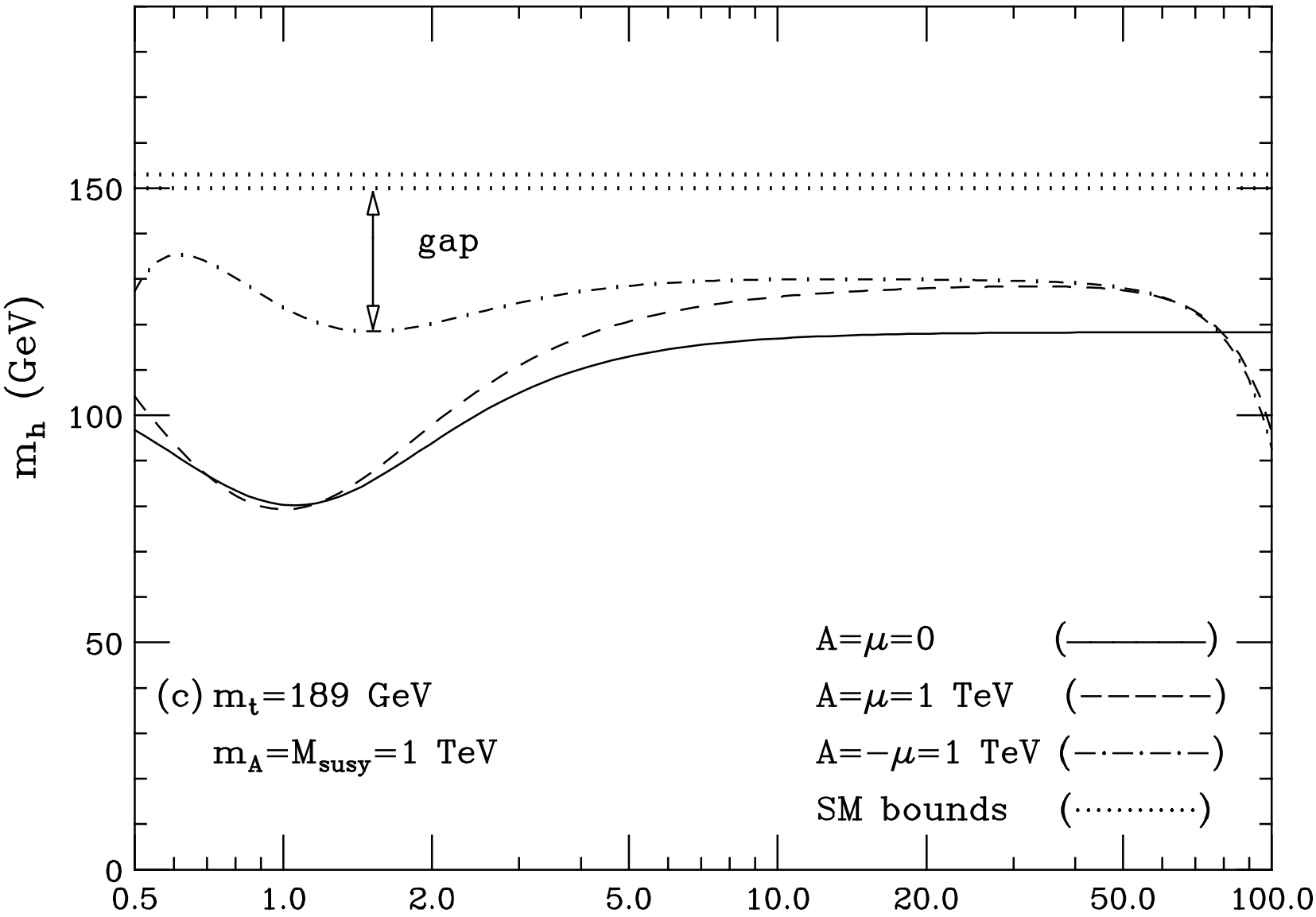
150
100
50
0
m_h (GeV)
gap
(c) m_t=189 GeV
m_A=M_{susy}=1 TeV
A=μ=0
A=μ=1 TeV
A=$-\mu$=1 TeV
SM bounds
0.5
1.0
2.0
5.0
10.0
20.0
50.0
100.0
tan β

Fig. 1(c)

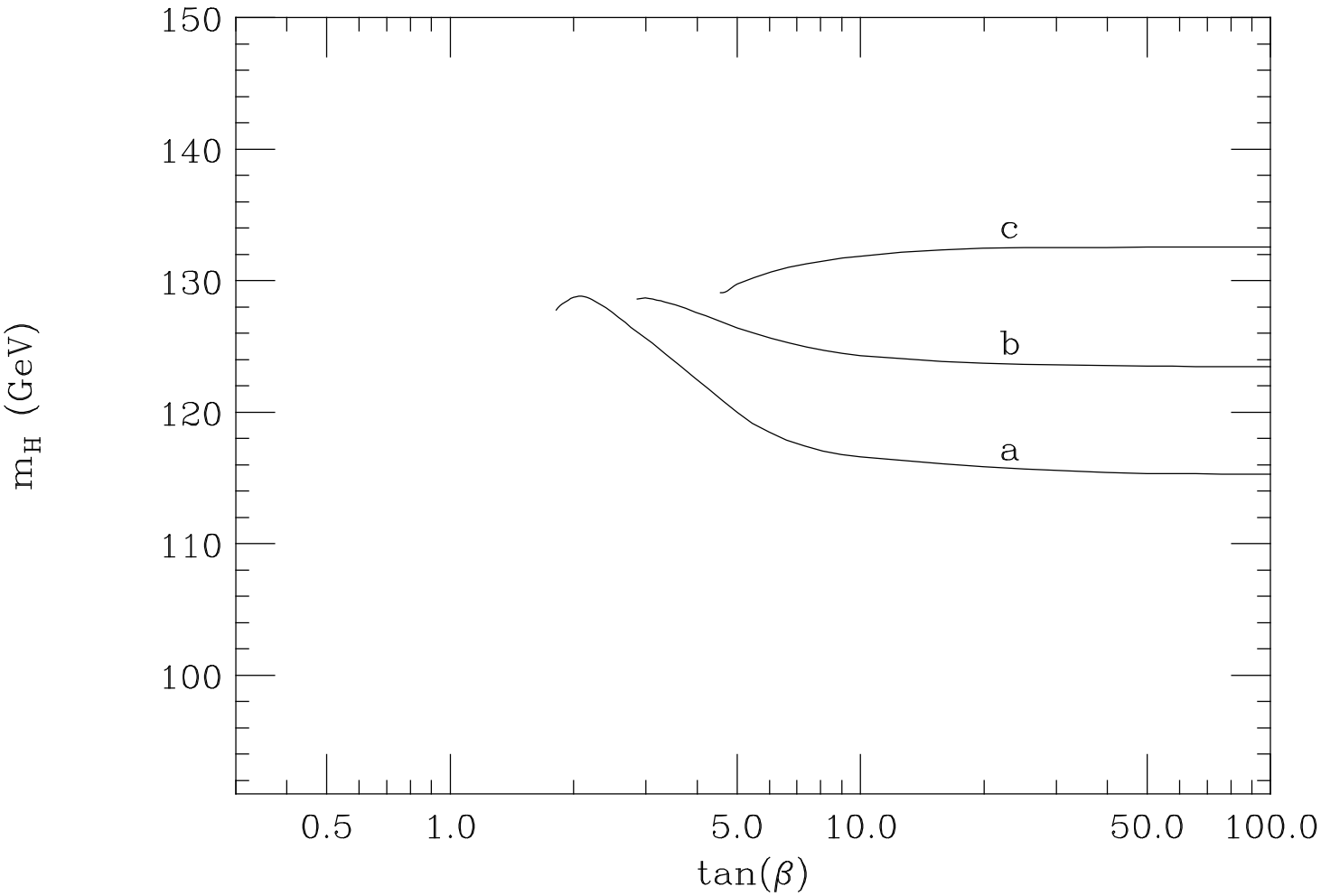
150
140
130
120
110
100
m_H (GeV)
c
b
a
0.5
1.0
5.0
10.0
50.0
100.0
tan(β)